A Thesis

On

Synthesis of Mn-Zn Ferrite Nanoparticles for Temperature Sensitive Magnetic Fluids

Submitted in partial fulfillment of requirement for the award of Degree of Master of Technology (M. Tech.)

In

MATERIALS AND METALLURGICAL ENGINEERING

Submitted by:

Ravi
(601102006)

Under the Supervision of

Dr. Bhupendrakumar Chudasama
(Assistant Professor)

School of Physics and Material Science
Thapar University
Patiala- 147004
INDIA

July 2013

“This thesis is dedicated to my parents and my loving sister
For their endless love, support and encouragement”

CERTIFICATE

This is to certify that **Mr. RAVI, Roll No. 601102006** has worked on this thesis report entitled **"Synthesis of Mn-Zn ferrite nanoparticles for temperature sensitive magnetic fluids"** as a partial fulfillment for award of the degree of MASTER OF TECHNOLOGY in Materials and Metallurgical Engineering. I certify that the matter embodied in this report is of the candidate's own record and not submitted to any other university in any part or full form for the award of such kind of a degree.

(Dr. Bhupendrakumar Chudasama)
Assistant Professor and Research Supervisor
School of Physics and Material Science
Thapar University
Patiala- 147004

Countersigned by:

(Dr. Kulvir Singh)
(Professor and Head)
School of Physics and Material Science
Thapar University, Patiala

(Dr. S.K. Mohapatra)
Dean of Academic Affairs
Thapar University, Patiala

ACKNOWLEDGEMENT

This master thesis was done in the School of Physics and Material Science, in the Thapar University and I wish to dedicate a few lines to thank every person who has helped and encouraged me during my thesis.

Foremost, I would like to express my sincere gratitude to my advisor Dr. Bhupenderakumar Chaudasama for the continuous support of my M. Tech. study and research, for his patience, motivation, enthusiasm, and immense knowledge. His guidance helped me in all the time of research and writing of this thesis. I could not have imagined having a better advisor and mentor for my M. Tech. thesis.

My sincere thanks also go to Dr. Nidhi Andhariya for useful discussion and helpful feedback. I am sure the knowledge gained through my association with her shall go a long way in the helping me to achieve success in my life.

I would like to express my sincere regard to Dr. Kulvir Singh, Head, School of Physics and Material Science for providing me necessary infrastructure facility for carrying out this work.

Besides my advisor, I would like to thank the rest of my teachers Dr. O.P. Pandey, Dr. K. K. Raina, Dr. N.K. Verma, Dr. Puneet Sharma, for their encouragement, insightful comments and good advice.

I would like to convey my special thanks to Ms. Chandni Khurana for her patience in laboratory and for reading this work with an external eye and for supporting me in the stress of the last weeks.

I would like to thank all my fellow classmates for the stimulating discussions, for the sleepless nights we were working together before deadlines, and for all the fun we have had in the last two years.

Ravi

(Ravi)

TABLE OF CONTENTS

LIST OF FIGURES

LIST OF TABLES

ABSTRACT

The main aim of this thesis is to prepare stable, magnetic fluid using Mn-Zn ferrite nanoparticles transformer cooling applications. In the present work magnetic nanoparticles $Mn_XZn_{(1-X)}Fe_2O_4$ (where x = 0, 0.2, 0.4, 0.6, 0.8,1) were successfully synthesized by Chemical Coprecepitation method. Experimental conditions have been established to prepare superparamagnetic, single phase Mn-Zn ferrite nanoparticles with desired chemical, physical and magnetic properties. By using oleic acid as surfactant, sterically stabilized extra pure kerosene based magnetic fluid is being produced. As-synthesized magnetic nanoparticles were characterized by X-ray diffraction (XRD), Transmission electron microscope (TEM), Vibrating sample magnetometer (VSM) and thermogravimetric (TGA) analysis. From the x-ray analysis, it is clarify evidenced that nanoparticles are crystallized into the well known inverse spinel structure. The peak broading is a clear indicative of formation of ultra small nanoparticles, which was further confirmed by transmission electron microscopy. Superparamagnetic nature of nanoparticles is confirmed via VSM measurement. TGA study confirms the monolayer coating on the surface of the nanoparticles which is essential for their stability in magnetic fluids. The magnetic nanoparticles produced here can be used in heat transfer devices.

CHAPTER 1

1 INTRODUCTION

1.1 NANOTECHNOLOGY

"*The principles of physics, as far as I can see, do not speak against the possibility of maneuvering things atom by atom. It is not an attempt to violate any laws."* these are the words which buried the seed for nanotechnology in the scientific mind of number of researchers who were attending the talk of famous physicist Richard Feynman in 1959 [1]. The word actually signifies our complete control over the matter. A nanometer is one billionth or 10^{-9}m. Nanotechnology makes us to believe that we would have the ability to create anything that we could precisely define. Eric Drexler [2], in the early 1980′s coined the powerful word nanotechnology. The world of nanotechnology is implanting its footprint in the present decade very rapidly. Between year 1997 and 2005, investment in nanotechnology research and development by governments around the world lift from $432 million to about $4.1 billion and corresponding industry investment exceeded that of governments by 2005. By 2015, products incorporating nanotechnology will contribute approximately $1 trillion to the global economy. About two million workers will be employed in nanotech industries. [3]

1.2 MAGNETISM

Magnetism is the phenomenon in which materials assert an attractive or repulsive force. However, the underlying principles and mechanisms that explain the magnetic phenomenon are complex and their understanding has eluded scientists until relatively recent times. Many of our modern technological devices rely on magnetism and magnetic materials; these include electrical power generators and transformers, electric motors, radio, television, telephones, computers, and components of sound and video reproduction systems. Basic concept of magnetic properties of a material is a result of interactions between an external magnetic field and the magnetic dipole moments of the constituent atoms. Associated with each individual electron are both orbital and spin magnetic moments. Basically, three types of magnetism are well known which are diamagnetism, peramagnetism and ferromagnetism. [4]

1.3 SUPERPARAMAGNETISM

Superparamagnetism is a type of magnetism which occurs in small ferromagnetic or ferrimagnetic nanoparticles. In sufficiently small nanoparticles, magnetization can randomly flip direction under the influence of temperature. The typical time between two flips is called the Neel relaxation time. In the absence of an external magnetic field, when the time used to measure the magnetization of the nanoparticles is much longer than the Neel relaxation time, their magnetization appears to be in average zero, they are said to be in the superparamagnetic state. It is similar to paramagnetic. However, their magnetic susceptibility is much larger than paramagnets. [5]

1.3.1 NEEL-RELAXATION THEORY

Generally, ferromagnetic or ferrimagnetic material undergoes a transition to a paramagnetic state above its Curie temperature (T_c). But superparamagnetism is different from this transition since it occurs below the Curie temperature of the material. Superparamagnetism occurs in nanoparticles which has single magnetic domain. This is only possible when diameter of nanoparticles generally lies between 3–50 nm: this limit varies from material to material. Because of the nanoparticle's magnetic anisotropy, the magnetic moment has only two stable orientations anti parallel to each other, which is separated by an energy barrier. The stable orientations of nanoparticle are called the "easy axis". At finite temperature, there is a limited probability for the magnetization to flip and reverse its direction.

1.4 MAGNETIC FLUID

A magnetic fluid is a liquid which is strongly magnetized in the presence of a magnetic field. Magnetic fluids are colloidal suspension of superparamagnetic particles in a carrier fluid (either an organic solvent or water). Each tiny particle is thoroughly coated with a surfactant to inhibit clustering. The magnetic attraction of nanoparticles is weak enough that the surfactant's steric repulsion is sufficient to prevent magnetic agglomeration. Magnetic fluids usually do not retain magnetization in the absence of an externally applied field. Composition of a typical magnetic fluid is 5% magnetic solid, 10% surfactant and 85% base liquid, by volume. [6]

1.5 MAGNETIC NANOPARTICLES

1.5.1 FERRITES

Ferrites are the class of ferromagnetic material. The general formula of ferrite is $M_{2+}Fe_2O_4$, where M is a divalent ion of a transition metal such as Fe, Co, Ni, Mn, Cu or Zn. A range of magnetic properties can be obtained through the choice of M. Ferrites are the chemical compound consists of ceramic material with iron oxide. Many of them are magnetic materials and they are used to make magnet and ferrite cores for transformers.

1.5.2 TYPES OF FERRITES

In terms of their magnetic properties, the different ferrites are often classified as "**soft**" or "**hard**", which refers to their low or high magnetic coactivity. [7]

SOFT FERRITE

Soft ferrites have low coercivity. It means that material's magnetization can easily reverse direction without dissipating much energy (hysteresis losses), while the material's high resistivity prevents eddy currents in the core, another source of energy loss. Because of their comparatively low losses at high frequencies, they can be use in the cores of RF transformers and switched-mode power supplies applications. The most common soft ferrites are the following:

- **Manganese-zinc ferrite** (**Mn-Zn**, with the formula $Mn_{x.}Zn_{(1-x).}Fe_2O_4$)
- **Nickel-zinc ferrite** (**Ni-Zn**, with the formula $Ni_{x.}Zn_{(1-x)}Fe_2O_4$).

1.5.3 Mn-Zn FERRITE

Magnetically responsive fluid having Mn–Zn ferrite nanoparticles is a probable contender for heat transfer applications. Magnetic fluids, whose magnetization strongly depends on temperature, when heated in a non-uniform magnetic field influences magnetic convection in addition to natural convection caused by an inhomogeneous distribution of fluid density in a temperature gradient. Thermo-magnetic energy conversion using magnetic fluid proposed during the early stage of the magnetic fluid research can be realized only by the synthesis of fluids having large paramagnetic coefficient. Only close to the Curie temperature the adiabatic magnetization can cause a considerable change in fluid temperature. In order to

tune the Curie temperature close to the operating range and to prepare a temperature-sensitive magnetic fluid, Mn - Zn nanoparticles can be used. The size of nanoparticles should be around 10 nm. [8]

1.5.4 STRUCTURE OF MAGNETIC NANOPARTICLES

The spinal structure is the most well known and useful example of MNP's. The spinal structure was named after mineral spinals ($MgAl_2O_4$) and can be represented as M' and M"2 X4. Where X represents oxygen anions and M' and M" are metallic ions. The crystallographic structure is formed by a nearly closed packed FCC array of anions with two unequivalent sites for cations. These differ in oxygen coordination; four oxygen ions surround tetrahedral cationic sites and octahedral sites by six oxygen ions. These are also called A- and B- sites respectively. In a cubic unit cell, 64 tetrahedral sites and 32 octahedral sites are present, out of which only 8 and 16 sites are occupied by metal ions respectively. A perfectly normal spinel is one in which the single A cation of the formula unit occupies the tetrahedral site, and the two B cation the two equivalent octahedral sites. If we designate the parentheses ( ) and [ ] to denote these two types of sites, then this distribution may be written as $(A).[B_2].O_4$. [9] The tetrahedral points are smaller than octahedral points. B^{3+} ion occupies the octahedral holes because of charge factor but can occupy half of the octahedral holes. A^{2+} occupies 1/8 of tetrahedral holes. However, the alternative distribution $(B).[AB].O_4$ is also possible. This arrangement is referred to as inverse spinal structure. An inverse spinal structure is an alternative arrangement where half of the trivalent ions swap with divalent ions. If A^{2+} ions have a strong preference for the octahedral site, they will force their way in to it and displace half of the B^{3+} from octahedral site to tetrahedral site. If B^{3+} ions have low or zero octahedral sites stabilization energy, then have no option and will adopt the tetrahedral site. The crystal field stabilization energy (CFSE) is highly useful to determine whether a structure would be normal or inverse. So we can say that if M^{3+} ion has higher CFSE in an octahedral field compared to M^{2+} ion, **normal spinal** result. If M^{2+} ion has a lower CFSE in an octahedral field compared to M^{3+} ion, **inverse spinal** result. [10]

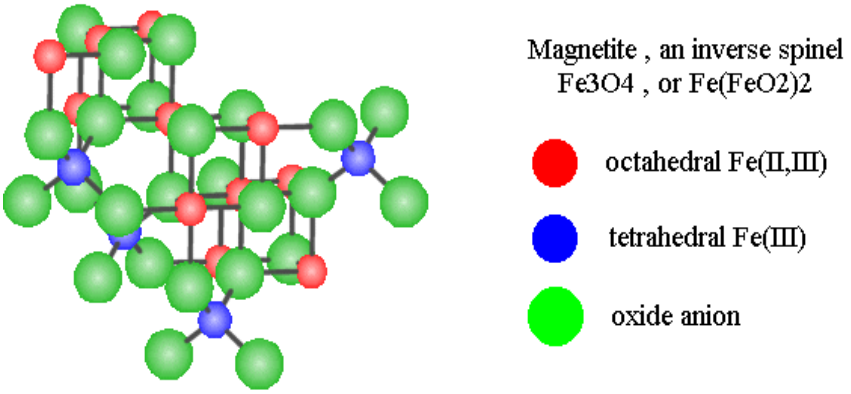

Figure 1.1 Inverse Spinal structure of Fe_3O_4

1.6 SURFACTANT

Surfactants are the compounds that lower the surface tension of a liquid. Surfactants may act as detergents, wetting agents, emulsifiers, foaming agents, and dispersants. The surfactant coats the magnetic nanoparticles in order to make colloidal suspension stable. To prevent agglomeration of nanoparticles, they are either coated with surfactant which will produce entropic repulsion or the surface of the nanoparticles is charged in order to achieve electrostatic repulsion. Oleic acid is one of the most widely used surfactants for electrostatic stabilization. [11]

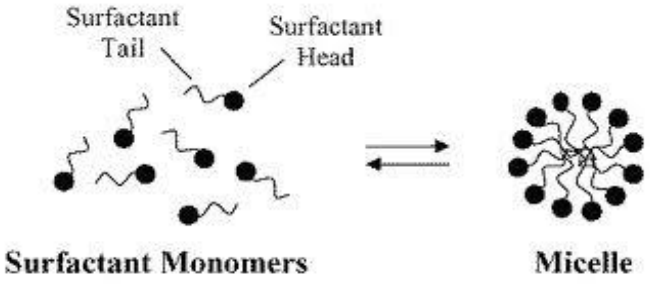

Figure 1.2 Schematic structures of a surfactant molecule and its micellar form

1.7 TYPES OF MAGNETIC FLUID

Magnetic fluids can be divided into two categories on the basis of surfactant.

1) Surfacted magnetic fluid
2) Ionic magnetic fluid

1.7.1 SURFACTED MAGNETIC FLUID

We know that surfactant is a detergent like substance in which one end of the molecule attaches to the surface of the particle, whereas the other end is more attracted to the liquid. This achieves a single layered polymer coating that prevents the agglomeration of magnetic nanoparticles. This process has the added benefit of making the magnetic material more lipids soluble, thus increasing the variety of carrier fluids that can be used. This is the preferred method of manufacturing commercial magnetic fluid. [12]

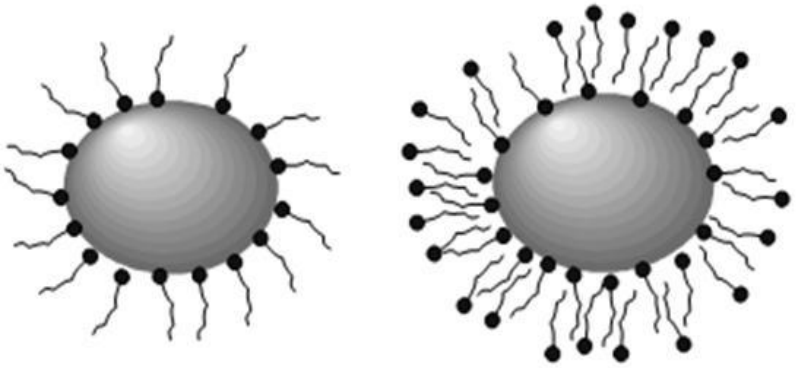

Figure 1.3 Surfacted magnetic fluids grains: (a) Single-layered grains (b) Double-layered grains

1.7.2 IONIC MAGNETIC FLUID

This process of making ionic fluid is easiest method of production. An easy and convenient chemical synthesis of ionic magnetic fluid was proposed in the early 80s: fine particles are precipitated and then peptized using an appropriate particle surface treatment. Like one simply collects sediment from a solution of iron salts, for eg. ferrous chloride ($FeCl_2$) or ferric chloride ($FeCl_3$). Electrostatic repulsion keeps the magnetic dipoles from getting close enough to each other and prevents agglomeration. This is the preferred method of synthesizing homemade magnetic fluids due to its simplicity & easy availability of materials. [12]

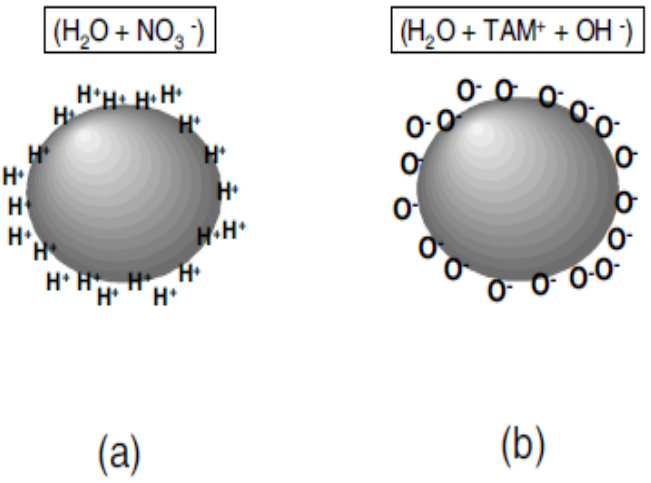

Figure 1.4 Representation of ionic magnetic fluid particles. a) Acid, magnetic fluid particle b) Alkaline magnetic particle, $TAM^{+}OH^{-}$ is tetra methyl ammonium hydro oxide

1.8 TRANSFORMER COOLING USING MAGNETIC FLUID

High-voltage power transformers are usually cooled by surrounding them with oil. As the oil is heated, it experiences a decrease in density; accordingly, oil in contact with the transformer coils absorbs the greatest amount of heat and, as a result, becomes least dense and raises relative. To the surrounding oil as the rising oil makes contact with the walls of the housing it transfers heat, cooling and increasing in density. The cooled oil travel toward the bottom of the container, replacing heated oil raising from the windings this natural convection caused by the interplay of gravity and heat induced density variations, represents the cooling mechanism most commonly utilized in high transformers. Unfortunately, the gravitational forces that circulate the oil are relatively weak. Temperature gradients across oil reservoirs are often observed to be quite large, signifying relatively poor heat transfer. So, to improve this heat transfer a magnetic field has been used for instead of oil surrounds the windings and core of transformer. The "leakage" field occurs as a result of electrical currents in the windings, and reflects imperfect channeling of the magnetic flux into the core; its strength is greatest in the immediate vicinity of the windings and core, and falls off rapidly with increasing distance. An electromagnetic device is immersed in a magnetic fluid, and the magnetic field gradient draws the magnetic fluid toward the device; however, because the device generates heat, the temperature of the fluid rises as it approaches the device, resulting in loss of magnetic properties and a decrease in density. The magnetic fluid rises as the gravitational effect of density reduction begins to overcome the weakening magnetic attraction. Movement of hot magnetic fluid is

assisted by the attraction exerted by the electromagnetic device on cooler, more intensely magnetic fluid which displaces the hot rising magnetic fluid as it travels toward the device. Movement away from the heat source and contact with the walls of the housing causes the hot fluid to cool and reacquire magnetization. This convection cycle driven by magnetic and gravitational forces, involves much faster fluid flows and therefore greater cooling effects than are achieved with ordinary systems. [13]

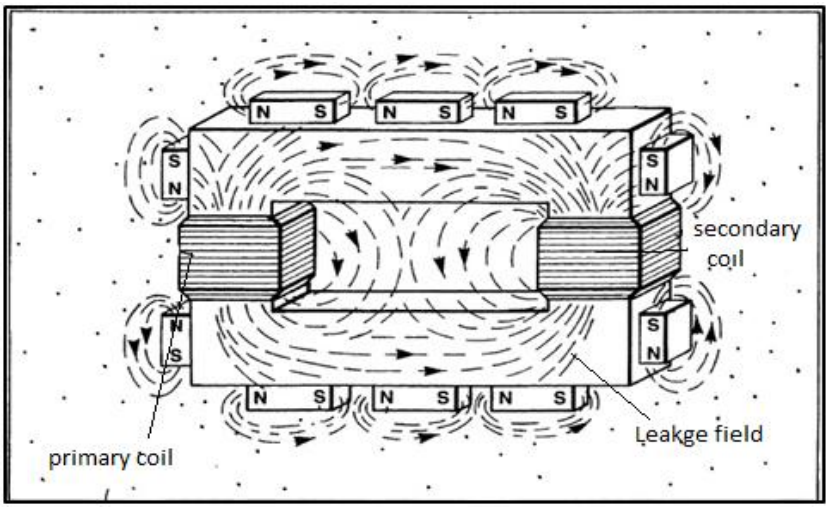

FIGURE 1.5 Mechanism of magnetic fluids cooling

CHAPTER 2

LITERATURE REVIEW

Ferro fluids were discovered in 1960's at NASA Research Centre. Scientists were exploring various techniques to control liquids in space when the solution in the form of a new idea of magnetic fluid emerged. It was found that its location can be changed by applying magnetic field and magnetic field strength can be used to induce fluidity. Researchers have used ferromagnetic compounds (Cobalt, Iron) and magnetic materials (manganese, zinc ferrite) in making magnetic fluid. But the maximum research until today has been done on the fluids containing magnetite.

Marie-Paule Pileni [14] in 2001 described a new synthesis method for making ferrite nanocrystals. In this paper she described the different ways to make magnetic fluids from colloidal self assemblies (normal and reverse micelles) and described the preparation of both ferrite nanocrystals with various compositions and cobalt metal nanocrystals. Normal micelles were used and make it possible to fabricate nanocrystals differing by their size with, to a first approximation, similar surface composition. This synthesis method was compared to those usually developed to fabricate magnetic fluids. Another synthesis for making FCC cobalt nanocrystals has also described. The general behavior with respect to magnetic properties for nanocrystals with various sizes has described, because a large variety of ferrites were used.

Voit *et al.* [15] in 2001 studied the magnetic behavior of nano sized iron oxide particles coated with different surfactants (sodium oleate, PVA and starch) in a ferrofluid. The super paramagnetic iron oxide particles, synthesized by a controlled co-precipitation technique, were found to contain magnetite (Fe_3O_4) as a main phase with a narrow physical particle size distribution between 6 and 8 nm. The mean effective magnetic size of the particles in different ferrofluid systems were estimated to be around 4-5 nm which was smaller than the physical particle size. On a 10% dilution in the starch coated ferrofluid, there was a decrease in the blocking temperature.

C. Grob *et al.* [16] in 2002 discussed the characterization of Magnetic fluid by Atomic force microscopy and photon correlation spectroscopy after magnetic fractionation. During magnetic fractionation the magnetic nanoparticles were separated according to their magnetic moments, as the magnetic moment of single domain of magnetic nanoparticles is proportional to amount of material. The AFM images show that the larger nanoparticles are

mostly agglomerates of smaller nanoparticles. It can be ruled out, that these agglomerates had been formed during the fractionation process or that they are artifacts derived from the preparation of the AFM samples. He told that the strength of the magnetic moment of the nanoparticles composed of one magnetic core will be independent of the external magnetic field, only its orientation will be influenced by the external field. Therefore, in applications where no or only weak external magnetic fields will be applied, the nanoparticles composed of several magnetic cores will not provide a magnetic force, whilst in applications where strong magnetic fields are applied, the two nanoparticles will yield comparable magnetic forces.

Patel *et al.* [17] in 2004 studied about the rheology of transformer oil based magnetic fluid. They reported that the result of rheological properties of temperature sensitive oil based ferrofluid as a function of external magnetic fluid and temperature. The field induced viscosity was analyzed by Shilomis method. The variation of magnetic moment and domain magnetization with temperature had been deduced from the measurement which agrees with reported valves deduced from magnetizations technique.

Kim *et al.* [18] in 2007 worked on formation and surface modification of Fe_3O_4 nanoparticles by Co-Precipitation and sol gel method. Fe_3O_4 nanoparticles were synthesized by Co-precipitation of Fe^{3+} and Fe^{2+} with NH_4OH and then silica was coated onto the surface of Fe_3O_4 by hydrolysis of TEOS (tetraethyl ortho silicate). Coupling agent was also coupled with the surface of the nanoparticles and protein was immobilized. Morphology, particle size, and magnetic properties of the nanoparticles were characterized by TEM, DLS, and VSM, respectively. As a result, silica coated Fe_3O_4 nanoparticles with an average size of 15 nm were obtained and super-paramagnetic properties were achieved.

Maity *et al.* [19] in 2007 worked on the magnetic fluids. The particles have been suspended in non-aqueous and aqueous media by coating the particles with a single layer and a bilayer of oleic acid, respectively. The particle sizes, morphology and the magnetic properties of the particles and the ferrofluid prepared from these particles were reported. The average particle sizes obtained from the TEM micrographs were 14, 10 and 9 nm for the water, kerosene and Dodecanese-based ferrofluid, respectively, indicating a better dispersion in the non-aqueous media. The specific saturation magnetization value of the oleic-acid-coated particles (53 emu /g) was found to be lower than that for the uncoated particles (63emu/g).

Zahn [20] in 2001 worked on magnetic fluid that magnetic field based micro/nano electromechanical systems devices were proposed that use 10 nm diameter magnetic particles, with and without a carrier fluid, for a new class of nano duct flows, nano motors, nano generators, nano pumps, nano actuators, and other similar nano scale devices. Ferro fluids which were synthesized as a stable colloidal suspension of permanently magnetized particles such as magnetite of 10 nm diameter were an excellent choice for such magnetic field technology. Brownian motion keeps the 10 nm size particles from settling under gravity, and a surfactant is placed around each particle to provide short range steric repulsion between particles to prevent particle agglomeration in the presence of non-uniform magnetic fields.

Desai *et al.* [21] in 2009 worked on structural and magnetic properties of $Mn_{0.5}Zn_{0.5}Fe_2O_4$ nanoparticles and magnetic fluid. They told that $Mn_{0.5}Zn_{0.5}Fe_2O_4$ ferrite nanoparticles with tunable Curie temperature and saturation magnetization were synthesized by using hydrothermal co-precipitation method. Particle size was controlled in the range of 54 to 135 Å by pH and incubation time of the reaction. All the particles exhibit super-paramagnetic behavior at room temperature. Langevin's theory incorporating the inter particle interaction was used to the virgin curve of particle magnetization. The low-temperature magnetization follows Bloch spin wave theory. Curie temperature derived from magnetic thermo gravimetric analysis showed that Curie temperature increases with increasing particle size. Using these particles magnetic fluid was synthesized and magnetic characterization was reported. The monolayer coating of surfactant on particle surface is confirmed using thermo gravimetric measurement. The same technique can be extended to study the magnetic phase transition.

Arulmurugun *et al*. [8] in 2006 worked on $Mn_{1-x}Zn_xFe_2O_4$ (with x varying from 0.1 to 0.5) ferrite nanoparticles used for ferrofluid preparation had been prepared by chemical co-precipitation method and characterized. Characterization techniques like elemental analysis by atomic absorption spectroscopy and spectrophotometers, thermal analysis using simultaneous TG-DTA, XRD, TEM, VSM and Mossbauer spectroscopy have been utilized. The final cation contents estimated agree with the initial degree of substitution. The Curie temperature (T_c) and particle size decrease with the increase in zinc substitution. In the case of particles with higher zinc concentration, both ferrimagnetic nanoparticles and particles exhibiting super paramagnetic behavior at room temperature are present. The fine particles were suitably dispersed in heptanes using oleic acid as the surfactant. They suggested that the volatile nature of the carrier chosen helps in altering the number concentration of the

magnetic particles in a ferrofluid having $Mn_{0.5}Zn_{0.5}Fe_2O_4$ particles can be used for the energy conversion application utilizing the magnetically induced convection for thermal dissipation.

Li *et al.* [22] in 2011 synthesized magnetic nanoparticles in $FeCl_2$-$NaNO_3$-NaOH aqueous system under various initial Fe^{2+}/NO^{3-} molar ratios (α) and Fe^{2+}/OH^- molar ratios (β). In order to clarify the effects of the initial molar ratio of reactants on the reaction mechanism, they set $Fe^{2+}/NO^{3-}/OH^-$ molar ratio in 3:1:5 which led to the formation of magnetic nanoparticles mainly composed of magnetite (Fe_3O_4) and maghemite (γ-Fe_2O_3). The 36 nm sized γ-Fe_2O_3 and 413 nm sized Fe_3O_4 were obtained by changing the order in which $NaNO_3$ was added to a NaOH solution. These in vitro heat generations of the resulting magnetic nanoparticles in an agar phantom were measured under an alternating magnetic field (100 kHz, 23.9 kA/m). The temperature rise (ΔT) of the agar phantom for the 36 nm sized γ-Fe_2O_3 was 55°C in the first 140 s, with a concentration of 58 mg Fe/mL. They showed that it is possible to prepare MNP's with high heating efficiencies under optimal conditions using the present method.

Elahi *et al.* [23] in 2012 published paper on Co-precipitation synthesis, physical and magnetic properties of manganese ferrite powder. Magnetic manganese ferrite powder was synthesized via chemical co-precipitation techniques using metallic chlorides of manganese and iron. Sodium hydroxide (NaOH) base was used as precipitant agent. The calcinations were performed at 600°C for 5 h. The structural investigation of the prepared sample was performed with X-ray diffractometer (XRD) and scanning electron microscope (SEM). The crystallite size was 26.53 nm, calculated using Sherrer formula. Magnetic properties were studied by vibrating sample magnetometer (VSM) techniques at room temperature. The value of magnetic saturization 16.36 emu/g, is at B is equal to 6.7 kOe. Low area hysteresis curve showed that the material formed is of soft magnetic material which keeps much importance in magnetic memory purposes.

Kopcansky *et al.* [24] in 2010 said that the field induced aggregation of magnetic particles can significantly change the dielectric breakdown strength of magnetic fluids if the sizes of the aggregates are comparable with the distance between the electrodes of the measured gap. Regarding to the better heat transfer, provided by magnetic fluids, their application in power transformers may lead to the improvement of the operation of these devices. Doping with magnetic particles shaped similarly to the liquid crystal molecules, gives better exploration of ferro nematics in the applications where the magnetic field is necessary to control the orientation of the liquid crystal molecules. The magnetic nanoparticles together with anticancer drug taxol encapsulated into the polymer nano

spheres of spherical shape of mean diameter approximately 250 nm, which is a relevant size for intravenous administration were prepared and characterized. The functionalized spheres have 5-times lower toxicity in comparison with pure taxol and are suitable for magnetic drug targeting.

Raj *et al.* [13] in 1995 worked on ferrofluid cooled electromagnetic device and improved cooling method. They made a convection cooled electromagnetic device, such as a transformer, and methods of cooling that utilize a ferrofluid as a cooling medium. The device's leakage magnetic field, which can be augmented by auxiliary magnets, draws the ferrofluid toward the device. As the fluid approaches the device its temperature rises, resulting in loss of magnetic properties and a decrease in density. The ferro fluid rises as its temperature approaches the Curie point.

.

CHAPTER 3

EXPERIMENTAL TECHNIQUES

3.1 SYNTHESIS TECHNIQUES

Magnetic nanoparticles can be synthesized by two ways.

i) Top down process
ii) Bottom up process

3.1.1 TOP DOWN PROCESS

The top-down method transforms the material with an initial size of a few micrometers into nano-particles with a size of only 40–200 nm. Generally mechanical milling is used for this purpose.

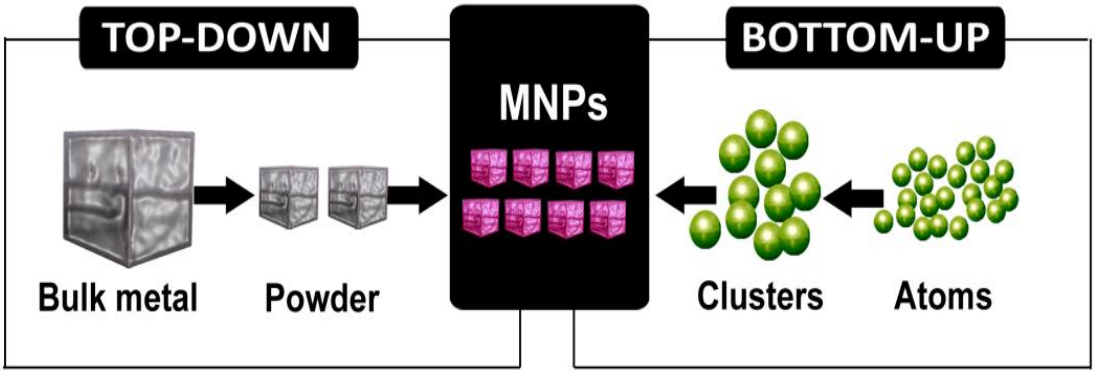

Figure 3.1 Schematic processes of Top down and Bottom up approach for the preparation of magnetic nanoparticles

3.1.2 BOTTOM UP PROCESS

The bottom-up method is used to generate the nanoparticles by heaping up atoms, or assemble the nanoparticles. It can produce nano-particles in any desired size. This method gives better nanostructures with fewer defects. Examples of bottom-up methods are:

i) Sol gel method
ii) Chemical vapor deposition
iii) Chemical co-precipitation, etc.

3.1.2.1 SOL-GEL METHOD

PRINCIPLE

Sol-gel technique becomes very popular recently due its high chemical homogeneity, low processing temperatures, and the possibility of controlling the size and morphology of particles. In this method, the 'Sol' (or solution) gradually evolves towards the formation of a Gel like diphase system containing both a liquid phase and solid phase whose morphologies range from discrete particles to continuous polymer networks. For example if we are to make magnetic nanoparticles, then iron solution is added to the citric acid solution drop wise with vigorous stirring. The solution was then heated to a temperature of 70^{o} C, while maintaining vigorous stirring until the gel was formed and the contained water was evaporated. The dried gel was then annealed at temperatures ranging from 180-400^{o} C, to get the nanoparticles. [25]

ADVANTAGES

1) It uses relatively low temperature.
2) It can create fine powder.
3) Easy to carry out the reaction.
4) It produces compositions not possible by solid-state fusion.

APPLICATIONS

1) One of the largest application areas is thin films and fibers.
2) Ultra-fine and uniform ceramic powders can be formed by this method.

3.1.2.2 CHEMICAL VAPOR DEPOSITION METHOD

PRINCIPLE

Chemical vapor deposition (CVD) is a chemical process used to produce high-purity, high-performance solid materials. The process is often used in the semiconductor industry to produce thin films. In a typical CVD process, a mixture of gases passing over a hot surface undergoes chemical reactions which lead to solid deposit on the surface. It is a complex phenomenon and is extremely versatile. Small changes in the experimental parameters cause

a drastic change in the results and hence lead to different branches of CVD. eg. Thermal CVD, plasma assisted CVD, Atmospheric pressure CVD, Low pressure CVD, The CVD is so rich and versatile because of its adaptability to new technologies. [26]

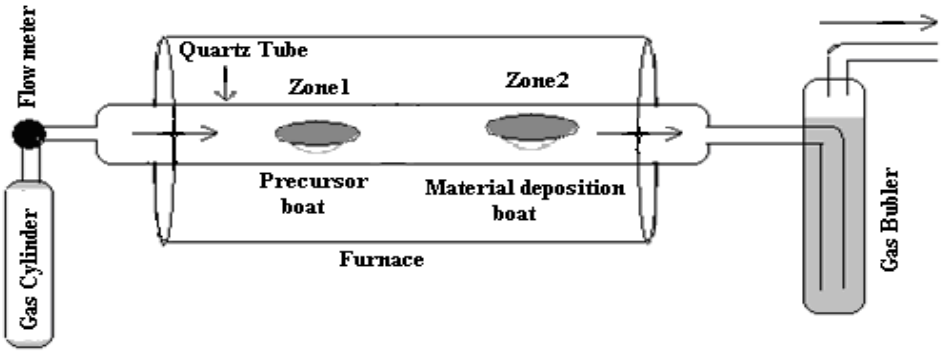

Figure 3.2 Schematic experimental setup of chemical vapor deposition method

3.1.2.3 CHEMICAL CO-PRECIPITATION METHOD

PRINCIPLE

The co-precipitation process is an extremely versatile method of producing ferrite nanoparticles with different size (3-20 nm) and magnetic properties prepared by simply controlling the experimental conditions. It is a facile and convenient way to synthesize iron oxides from aqueous $Fe^{2+/}Fe^{3+}$ salt solutions by the addition of a base under inert atmosphere at room temperature or at elevated temperature. The size, shape, and composition of the magnetic nanoparticles depends on the type of salts used (e.g. chlorides, sulfates, nitrates), the $Fe^{2+/}Fe^{3+}$ ratio, the reaction temperature, the pH value and ionic strength of the media. Once the synthesis conditions are established, the quality of the magnetite nanoparticles is highly reproducible. To produce substituted nano-sized ferrite particles suitable for use in magnetic fluids the Fe^{2+} ion is simply replaced or partially replaced by another or combination of divalent metal ions such as Co^{2+}, Mn^{2+}, Ni^{2+}, Zn^{2+}, etc.

Nanoparticle of $Mn_{(1-x)}Zn_xFe_2O_4$ with (x = 0, 0.2, 0.4, 0.8 and 1.0) were prepared by co-precipitation method. Requisite quantity of aqueous solution of $MnCl_2.4H_2O$ was mixed with aqueous solution of $ZnSO_4.7H_2O$. Color of the mixture was transparent. Now $FeCl_3.6H_2O$ dissolved in distilled water was added to the previous mixture under constant magnetic stirring. Upon the addition of $FeCl_3.6H_2O$, the color of the mixture immediately turned to light yellow. The pH of this mixture should be less than 2. We use

NaOH as co-precipitating agent. Mixed solution of $MnCl_2.4H_2O$, $ZnSO_4.7H_2O$ and $FeCl_3.6H_2O$ was added to the solution of NaOH within 10 sec under constant mechanical stirring. The color of this mixture turned dark brown. The pH of this mixture was adjusted to 10.5 with excess NaOH solution. Stir the mixture for 20 minutes. Nanoparticles were formed by conversion of metal salt in to hydroxide. Then the solution is heated up to 80°C up to 1 hour under constant mechanical stirring. The reaction mixture was magnetically decanted. After several water washes and acetone wash sample was dry in an oven at 82°C for 10-12 hours and then grinded with mortar and pestle. During synthesis, molar concentration, temperature and pH of reaction mixture were optimized to get single-phase nanoparticles. [27]

ADVANTAGES

- Easy control of particle size and composition.
- Time saving
- Inexpensive
- Processed at much lower temperature
- Various possibilities to modify the particle surface and overall homogeneity

CHEMICAL REACTIONS

Following reactions were taken place.

- $MnCl_2.4H_2O + 2\ FeCl_3.6H_2O + 8NaOH \rightarrow \mathbf{MnFe_2O_4} + 8NaCl + 20H_2O$
- $0.8\ MnCl_2.4H_2O + 0.2\ ZnSO_4.7H_2O + 2FeCl_3.6H_2O + 8NaOH \rightarrow \mathbf{Mn_{0.8}Zn_{0.2}Fe_2O_4} + 0.2Na_2SO_4 + 7.6NaCl + 20.6H_2O$
- $0.6\ MnCl_2.4H_2O + 0.4\ ZnSO_4.7H_2O + 2FeCl_3.6H_2O + 8NaOH \rightarrow \mathbf{Mn_{0.6}Zn_{0.4}Fe_2O_4} + 0.4Na_2SO_4 + 7.2NaCl + 21.2H_2O$
- $0.4\ MnCl_2.4H_2O + 0.6\ ZnSO_4.7H_2O + 2FeCl_3.6H_2O + 8NaOH \rightarrow \mathbf{Mn_{0.4}Zn_{0.6}Fe_2O_4} + 0.4Na_2SO_4 + 7.2NaCl + 21.2H_2O$
- $0.2MnCl_2.4H_2O + 0.8ZnSO_4.7H_2O + 2FeCl_3.6H_2O + 8NaOH \rightarrow \mathbf{Mn_{0.2}Zn_{0.8}Fe_2O_4} + 0.6Na_2SO4 + 6.8NaCl + 21.8H_2O$

• $ZnSO_4.7H_2O + 2FeCl_3.6H_2O + 8NaOH \rightarrow \mathbf{ZnFe_2O_4} + Na_2SO4 + 6NaCl + 23H_2O$

3.1.2.3.4 SYNTHESIS OF $MnFe_2O_4$ BASED MAGNETIC FLUID

PROCEDURE

1. 1.97 gram of $MnCl_2.4H_2O$ and 5.39 gm of $FeCl_3.6H_2O$ added in 200 ml water and 3.19 gm of NaOH was dissolved in 200 ml water.
2. Prepare the nanoparticles slurry as described in previous section.
3. Prepare 50 ml NaOH solution.
4. Add drop wise 2-3 ml Oleic acid in NaOH solution add the particle slurry into Oleic acid solution and heat the mixture at 93^o C for 2 minute with continues stirring.
5. Cool the reaction mixture to room temperature and foculate with dilute HCL.
6. Decant the solution by magnetic means and wash the nanoparticles with mild hot distilled water several times.
7. Give one acetone wash to remove residual water from the sample.
8. Add 25 ml extra pure kerosene into the nanoparticle slurry and heat it gently until the particles stands suspending into the solvent.
9. Check the stability of magnetic fluid with a permanent magnet.

3.2 CHARACTERIZATION TECHNIQUES

3.2.1 X-RAY DIFFRACTION

X-ray powder diffraction (XRD) is a powerful technique which is used for phase identification of a crystalline material and unit cell dimensions. The atomic planes of a crystal cause an incident beam of X-rays to interfere with one another as they leave the crystal. The phenomenon is called X-ray diffraction.

PRINCIPLE

X -ray diffraction is based on constructive interference of monochromatic X-rays from a crystalline sample. These X-rays are generated in a cathode ray tube, filtered to produce monochromatic radiation, collimated to concentrate, and directed toward the sample. The interaction of the incident rays with the sample produces constructive interference (and a diffracted ray) when conditions satisfy the Bragg's Law.

$$n\lambda = 2d \sin\theta$$

Where,

n= integer

λ= wavelength

d= spacing between plane in the atomic lattice

θ= angle between the incident ray and scattering plane

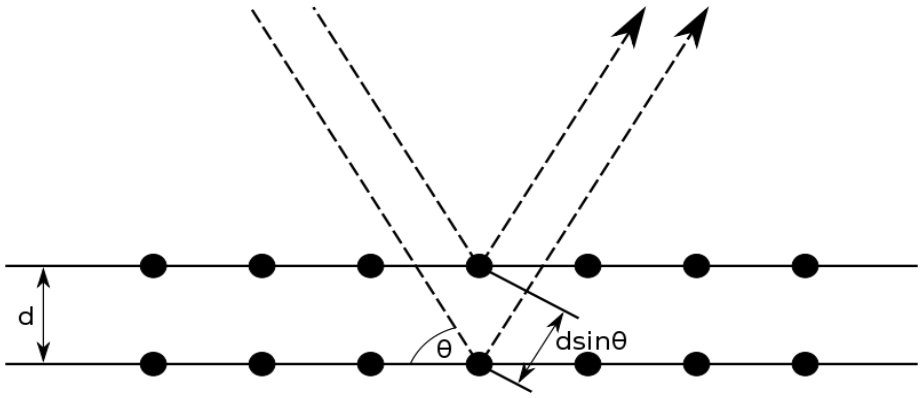

Figure 3.3 Represent Bragg diffraction, two beams with identical wavelength and phase approach a crystalline solid and are scattered.

BRAGG'S LAW

Bragg's Law was derived by physicist Sir William Lawrence Bragg in 1912. This law relates the wavelength of electromagnetic radiation to the diffraction angle and the lattice spacing in a crystalline sample. These diffracted X-rays are then detected, processed and counted. By scanning the sample through a range of 2θ angles, all possible diffraction directions of the lattice should be attained due to the random orientation of the powdered material. Conversion of the diffraction peaks to d-spacing allows identification of the mineral because each mineral has a set of unique d-spicing. Typically, this is achieved by comparison of d-spacing with standard JCPDF card.

WORKING

X-ray diffractometers consist of three basic elements: an X-ray tube, a sample holder, and an X-ray detector.

Figure 3.4 Represent the X-ray diffraction instrument

X rays are generated in a cathode ray tube by heating a filament to produce electrons, and accelerating the electrons toward a target by applying a voltage. When electrons have sufficient energy to dislodge inner shell electrons of the target material, characteristic X-rays are produced. These spectra consist of several components, the most common being K_{α} and K_{β}. K_{α} consists, in part, of $K_{\alpha 1}$ and $K_{\alpha 2}$. $K_{\alpha 1}$ has a slightly shorter wavelength and twice the intensity as $K_{\alpha 2}$. The specific wavelengths are characteristic of the target material (Cu, Fe, Mo, and Cr). $K_{\alpha 1}$and $K_{\alpha 2}$ is sufficiently close in wavelength such that a weighted average of the two is used. Copper is the most commonly used target material. These X-rays are collimated and directed onto the sample. As the sample and detector are rotated, the intensity of the reflected X-rays is recorded. When the geometry of the incident X-rays impinging the sample satisfies the Bragg's Equation, constructive interference occurs and a peak in intensity is obtained. A detector records and processes this X-ray signal and converts the signal to a count rate which is then output to a device such as a computer screen. [28]

APPLICATION

- The identification and characterization of unknown crystalline materials.
- Determination of unit cell dimensions
- Measurement of sample purity. XRD can also make texture measurement, such as the orientation of grain in polycrystalline samples.
- It can also determine the thickness, roughness and density of the thin film.

3.2.2 VIBERATING SAMPLE MAGNETOMETER (VSM)

A vibrational sample magnetometer or VSM is a scientific instrument which was invented in 1955 by Simon Foner at Lincoln Laboratory MIT. A vibrational sample magnetometer, measures the magnetic moment of a sample when it is vibrated perpendicularly to a uniform magnetizing field.

PRINCIPLE

A vibrating sample magnetometer (VSM) operates on Faraday's Law of Induction, which tells us that a change in magnetic field will produce an electric field. This electric field can be measured and provide information about the changing magnetic field. With this instrument, changes as small as 10^{-5} to 10^{-6} emu can be detected, and a stability of one part in 10^{4} can be attained. A VSM operates by first placing the sample to be studied in a constant magnetic field. If the sample is magnetic, this constant magnetic field will magnetize the sample by aligning the magnetic domains with the field. The stronger the constant field, the larger the magnetization will be. The magnetic dipole moment of the sample will create a magnetic field around the sample, sometimes called the magnetic stray field. As the sample is moved up and down, this magnetic stray field is changing as a function of time and can be sensed by a set of pick-up coils. The alternating magnetic field will cause an electric field in the pick-up coils according to Faraday's Law of Induction. This current will be proportional to the magnetization of the sample. [29]

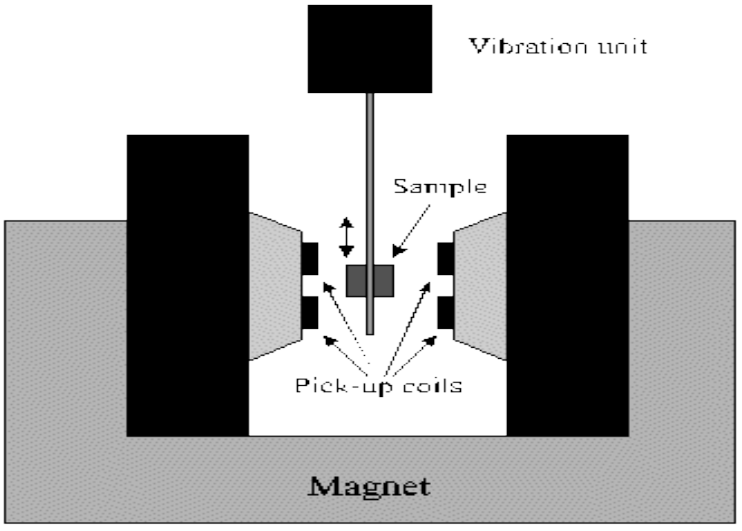

Figure 3.5 Representation of VSM set up

A typical measurement of a sample is taken in the following manner:

- The strength of constant field is set and sample begins to vibrate.
- The signal received from the probe is translated into a value for the magnetic moment.
- The strength of the constant magnetic field changes to a new value.
- The constant magnetic field varies over a given range, and a plot of magnetization (M) versus magnetic field strength (H) is generated.

APPLICATION

The vibrating sample magnetometer has become a widely used instrument for determining magnetic properties of a large variety of materials: diamagnetic, paramagnetic, ferromagnetic, and ferrimagnetic and anti ferromagnetic and give information about the hysteresis, saturation, coercivity and anisotropy.

3.2.3. TRANSMISSION ELECTRON MICROSCOPE (TEM)

PRINCIPLE

Transmission Electron Microscopy (TEM) is a vital characterization tool for the measurement of particle size, size distribution, and morphology. TEM operates on the same basic principles as the light microscope but uses electrons instead of light. The TEM has the added advantage of greater resolution. This enables the instrument's user to examine fine detail even as small as a single column of atoms, which is tens of thousands times smaller than the smallest resolvable object in a light microscope. At smaller magnifications TEM image contrast is due to absorption of electrons in the material, due to the thickness and composition of the material. At higher magnifications complex wave interactions modulate the intensity of the image, requiring expert analysis of observed images.

TEM has several components. Some of them are listed below.

Vacuum system: To increase the mean free path of the electron gas interaction, a standard TEM is evacuated to low pressures, typically on the order of 10^{-4} Pa. Vacuum is achieved with either a rotary vane pump or turbo molecular pump

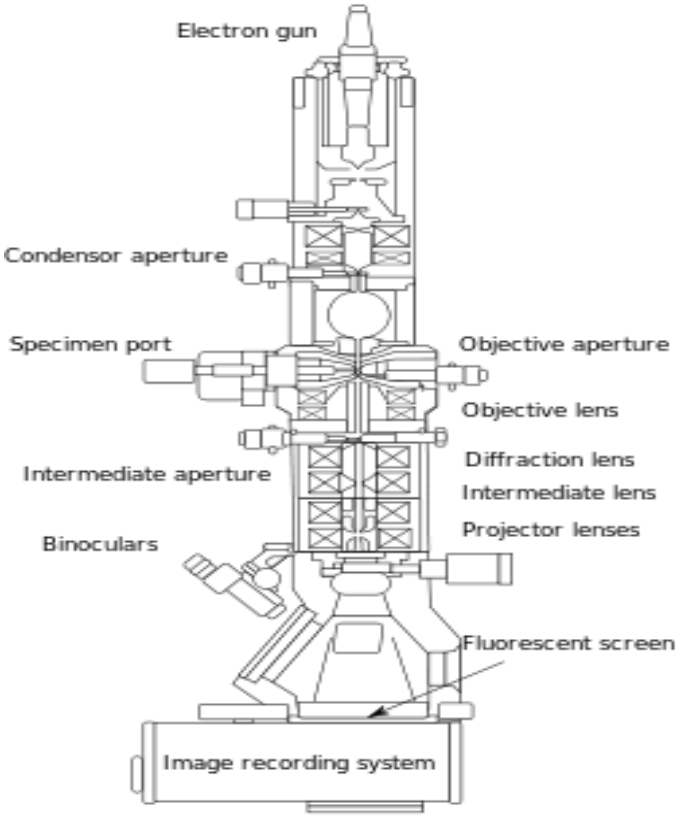

Figure 3.6 Schematic layouts of Transmission electron microscope

- **Specimen stage:** A TEM stage is required to have the ability to hold a specimen and be manipulated to bring the region of interest into the path of the electron beam.
- **Electron gun:** By connecting the filament to the negative component power supply, electrons can be pumped from the electron gun to the anode plate. This gun is designed to create a beam of electrons at any given angle.
- **Electron lens:** Electron lenses are designed to act in a manner similar to that of an optical lens, by focusing parallel rays at some constant focal length
- **Aperture:** A small metallic disc that is sufficiently thick to prevent electrons from passing through the disc. Apertures decrease the beam intensity as electrons are filtered from the beam, which may be desired in the case of beam sensitive samples.

WORKING

TEM consists of an emission source, which may be a tungsten filament, or a lanthanum hexaboride (LaB_6). For tungsten, this will be of the form of a hairpin-style filament. LaB_6 sources utilize small single crystals. By connecting this gun to a high voltage it will produce high current, and begin to emit electrons. This beam of electrons is transmitted

through an ultra-thin specimen, interacting with the specimen as it passes through. Due to this interaction an image is formed and then image is magnified and focused onto an imaging device, such as a fluorescent screen, on a layer of photographic film, or to be detected by a sensor such as a CCD camera. [30]

APPLICATION

- For morphological analysis
- For electronic diffraction
- For qualitative and semi-quantitative analysis.

3.2.4 THEMAL GARVIMETRIC ANALYSIS (TGA)

PRINCIPLE

Thermogarvimetric Analysis (TGA) measures the amount and rate of change in the weight of a material as a function of temperature or time in a controlled atmosphere. Measurements are used to determine the composition of materials and to predict their thermal stability at higher temperatures. The technique can characterize materials that exhibit weight loss or gain due to decomposition, oxidation, or dehydration.

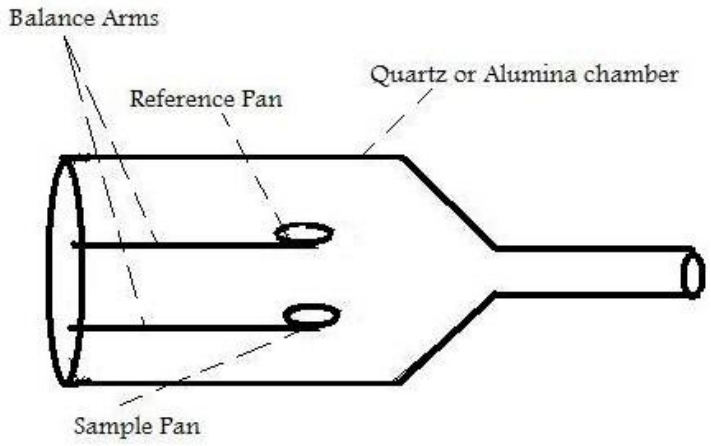

Figure 3.7 Represent the Thermal gravimetric analyzer

A TGA consists of a sample pan that is supported by a precision balance. That pan resides in a furnace and is heated or cooled during the experiment. The mass of the sample is monitored during the experiment. A sample cleaning gas controls the sample environment. This gas may be inert or a reactive gas that flows over the sample and exits through an

exhaust. As many weight loss curves look similar, the weight loss curve may require transformation before results may be interpreted. A derivative weight loss curve can identify the point where weight loss is most apparent. Thermogravimetric analysis uses heat to force reactions and physical changes in materials. [31]

APPLICATION

- To determine purity and thermal stability.
- To determine decomposition of inorganic and organic material
- To determine composition of metal
- Moisture content, etc.

CHAPTER 4

RESULT & DISCUSSION

4.1 XRD ANALYSIS

Structural characterization of magnetic nanoparticles was carried out by recording their powder XRD pattern. The pattern was recorded on X-ray diffractometer Bruker D8 Advance X-ray at room temperature using monochromatic radiation of CuKα (λ = 0.15406 nm). [32] Analysis of powders by XRD requires that they must be extremely fine grained to achieve good signal-to noise ratio, avoid spottiness and minimize preferred orientation. Grinding is accomplished by the mortar and pastel to make it homogenous. Nanoparticles are packed to a flat surface onto a sample holder to assume different orientations and ensure reflections from various hkl planes. The magnetic nanoparticles is analyzed for phase composition using X-ray powder diffraction over the 2 θ range from 10–80° at rate of 2°/min. Figure 4.1 shows the XRD pattern of $Mn_{(1-x)}Zn_XFe_2O_4$ nanoparticles where X varies from 0 to 1. It can be seen that diffraction peaks are consistent with the standard pattern for JCPDS card no. (73-1964).

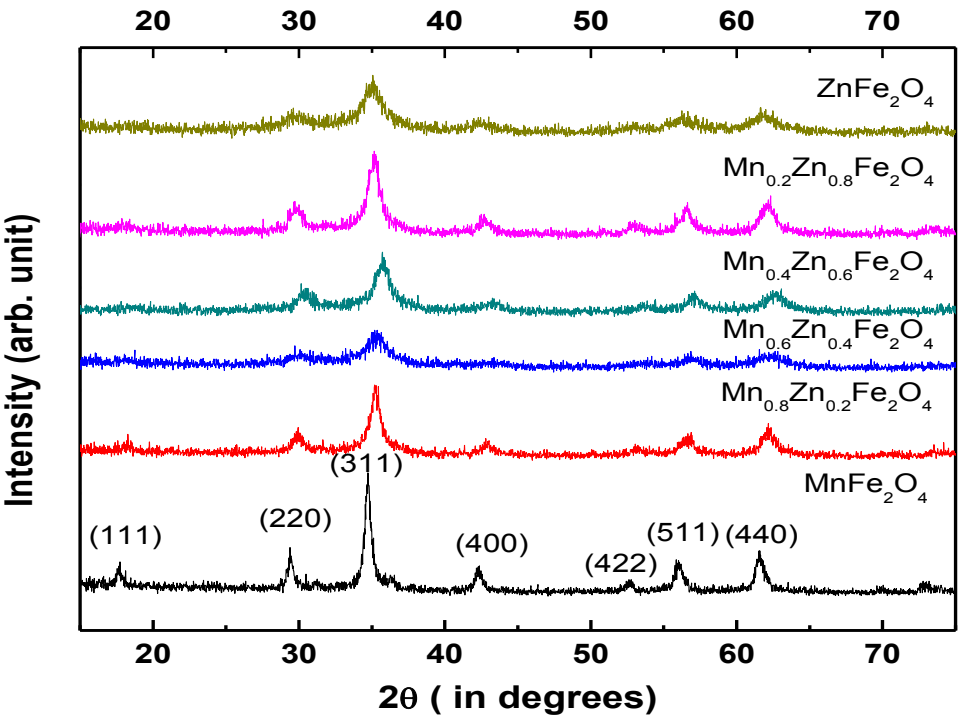

Figure 4.1 XRD pattern of $Mn_{(1-x)}Zn_xFe_2O_4$ **(**X=0, 0.2, 0.4, 0.6, 0.8, and 1**)** nanoparticles

The peak at 2θ = 17.713°, 29.551°, 37.794°, 42.312°, 52.78°, 55.98°, 61.668° can be attributed to (111), (220), (311), (400), (422), (511), (440) crystal planes of FCC structure

respectively. There is no extra peak which indicates that samples having crystallized in to single phase. The crystallite size can be calculated from the fitting of the highest intense peak (311) by Debye-Scherrer formula

$$D = \frac{0.9\lambda}{\beta cos\theta}$$

Where,

D = Crystallite size

λ = wavelength of X-ray source= 1.5406 Å

β = full width at half maximum (FWMH) of highest intense peak.

θ = Diffraction angle of highest intense reflection.

Crystallite size calculated for each sample is tabulated in table 4.1. The crystallite size was found to be in the range of 6-19 nm. Very small crystallite size of nanoparticles indicates that they may posse's superparamagnetic character. The lattice parameter "a" and interplaner distance "d_{hkl}" has been calculated by Bragg's law by using following equations.

$$d = \frac{\lambda}{2\sin\theta} \text{ and } \mathrm{d} = \frac{\mathrm{a}}{\sqrt{\mathrm{h}^2+\mathrm{k}^2+\mathrm{l}^2}}$$

Where,

d = interpalner spacing

a = lattice parameter

h, k, l are the miller indices.

Table 4.1 Interplaner spacing, lattice parameter, and crystallite size of $Mn_XZn_{(1-x)}Fe_2O_4$ (X=0, 0.2, 0.4, 0.6, 0.8, and 1) nanoparticles.

Sr. No.	Sample Code	Interplaner spacing "d_{hkl}"(Å)	Lattice parameter "a"(Å)	Crystallite Size D (nm)
1	$MnFe_2O_4$	2.34	8.42	18.45
2	$Mn_{0.8}Zn_{0.2}Fe_2O_4$	2.33	8.45	13.22
3	$Mn_{0.6}Zn_{0.4}Fe_2O_4$	2.68	8.38	7.09
4	$Mn_{0.4}Zn_{0.6}Fe_2O_4$	2.05	8.35	8.09
5	$Mn_{0.2}Zn_{0.8}Fe_2O_4$	1.96	8.39	10.46
6	$ZnFe_2O_4$	2.09	8.50	6.92

The calculated values of lattice parameter of as-synthesized samples are in well agreement with reported for JCPDS card number (73-1964) $MnFe_2O_4$. Little fluctuation in lattice parameter is due to the difficulties in determining peak position accurately for samples with increasing Zn content. Each sample has a cubic spinal ferrite phase with good crystallinity.

4.2 VSM ANALYSIS

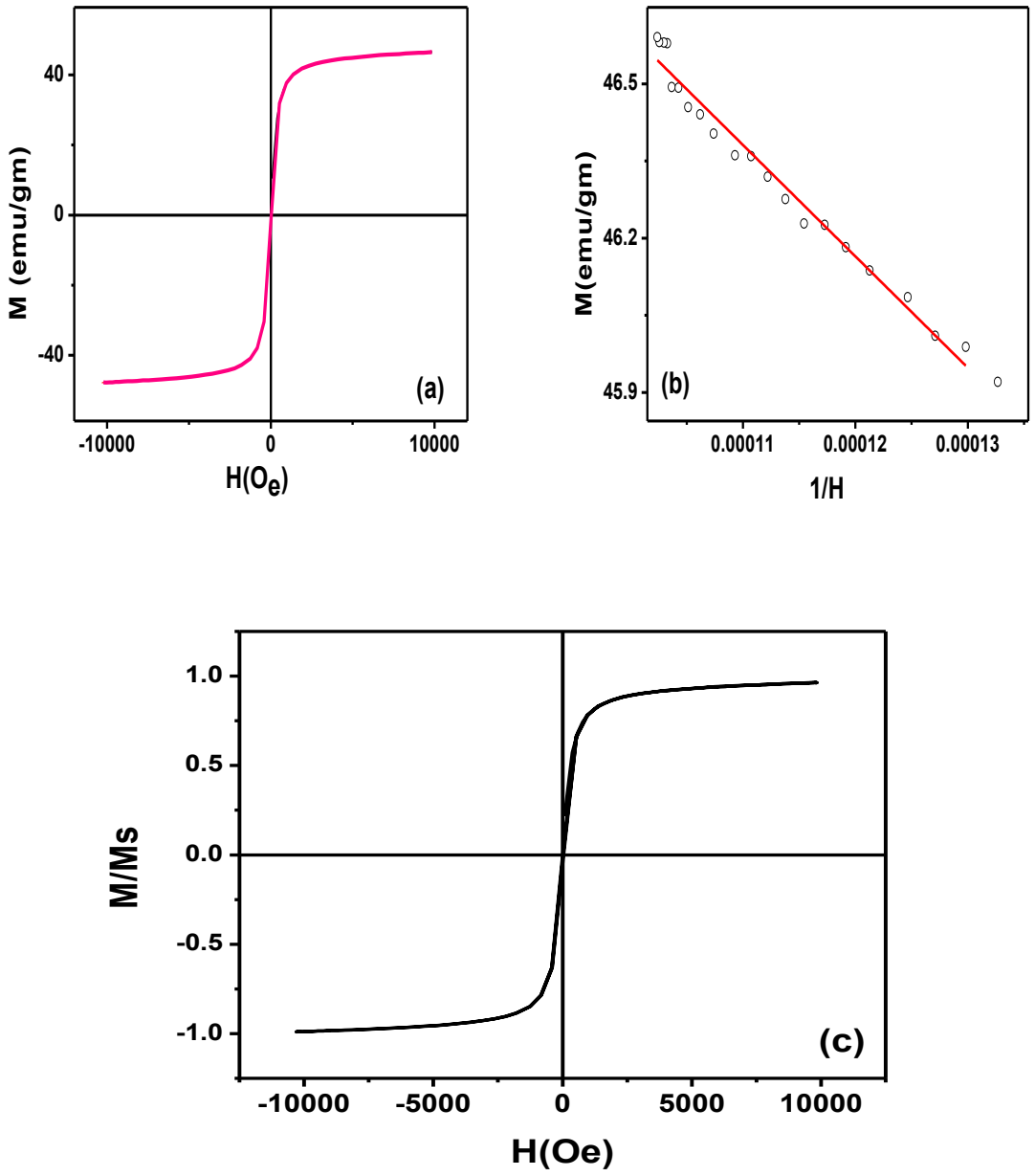

Figure 4.2 (a) M–H hysteresis **(b)** M–1/H and **(c)** M/Ms–H curves of $MnFe_2O_4$ nanoparticles

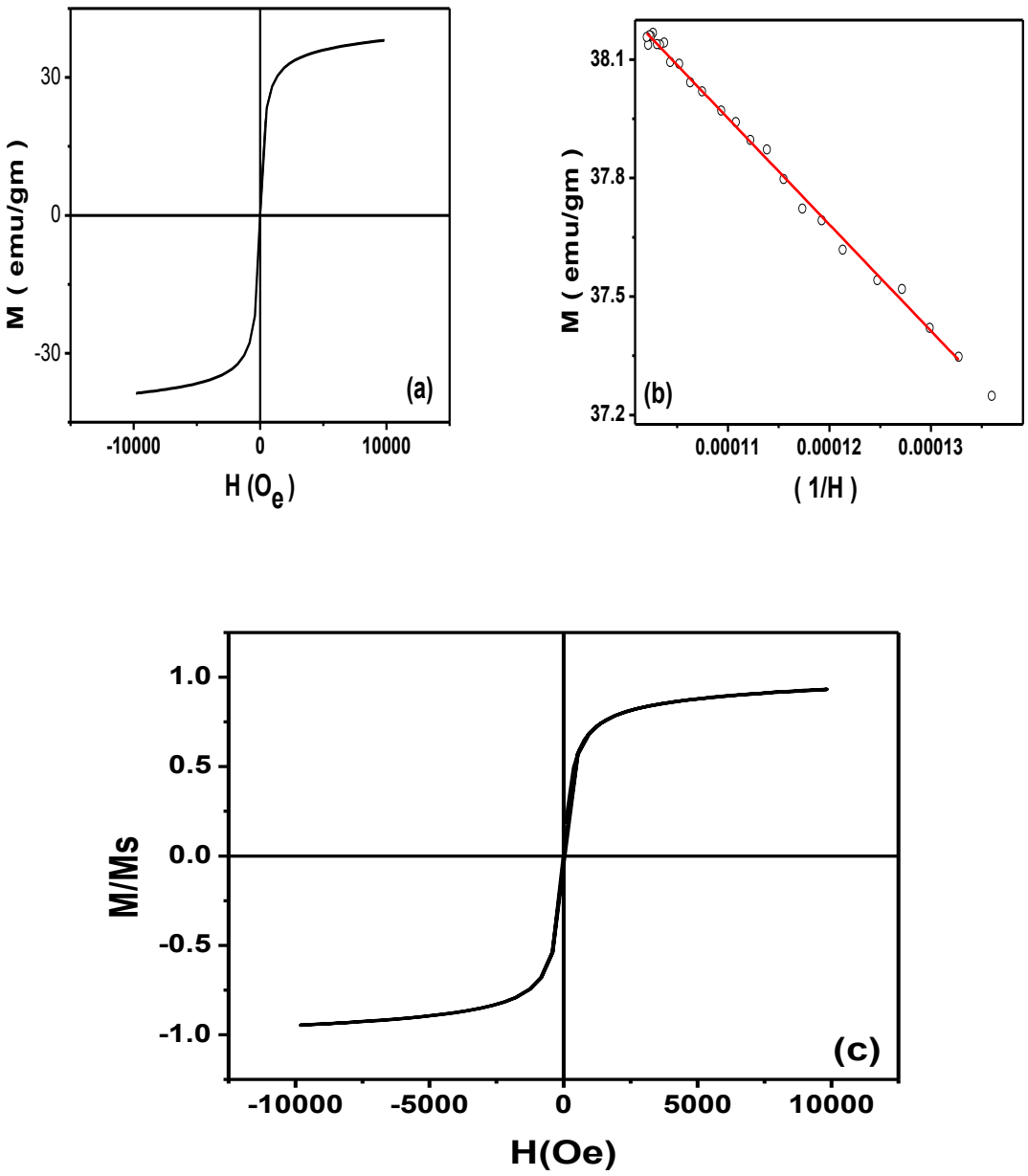

Figure 4.3 (a) M–H hysteresis **(b)** M – 1/H and **(c)** M/Ms–H curves of $Mn_{0.8}Zn_{0.2}Fe_2O_4$ nanoparticles

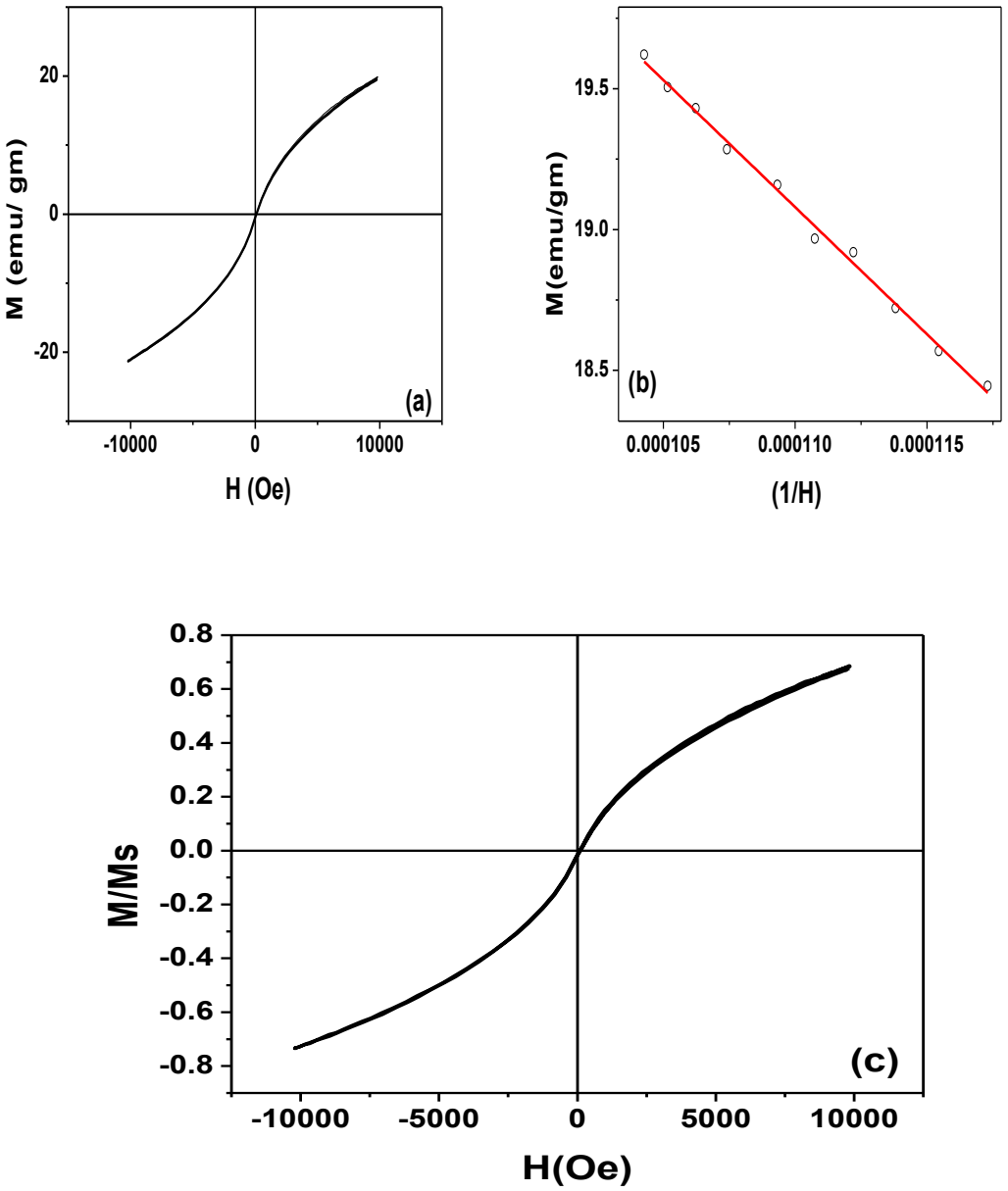

Figure 4.4 (a) M–H hysteresis **(b)** M–1/H and **(c)** M/Ms–H curves of $Mn_{0.6}Zn_{0.4}Fe_2O_4$ nanoparticles

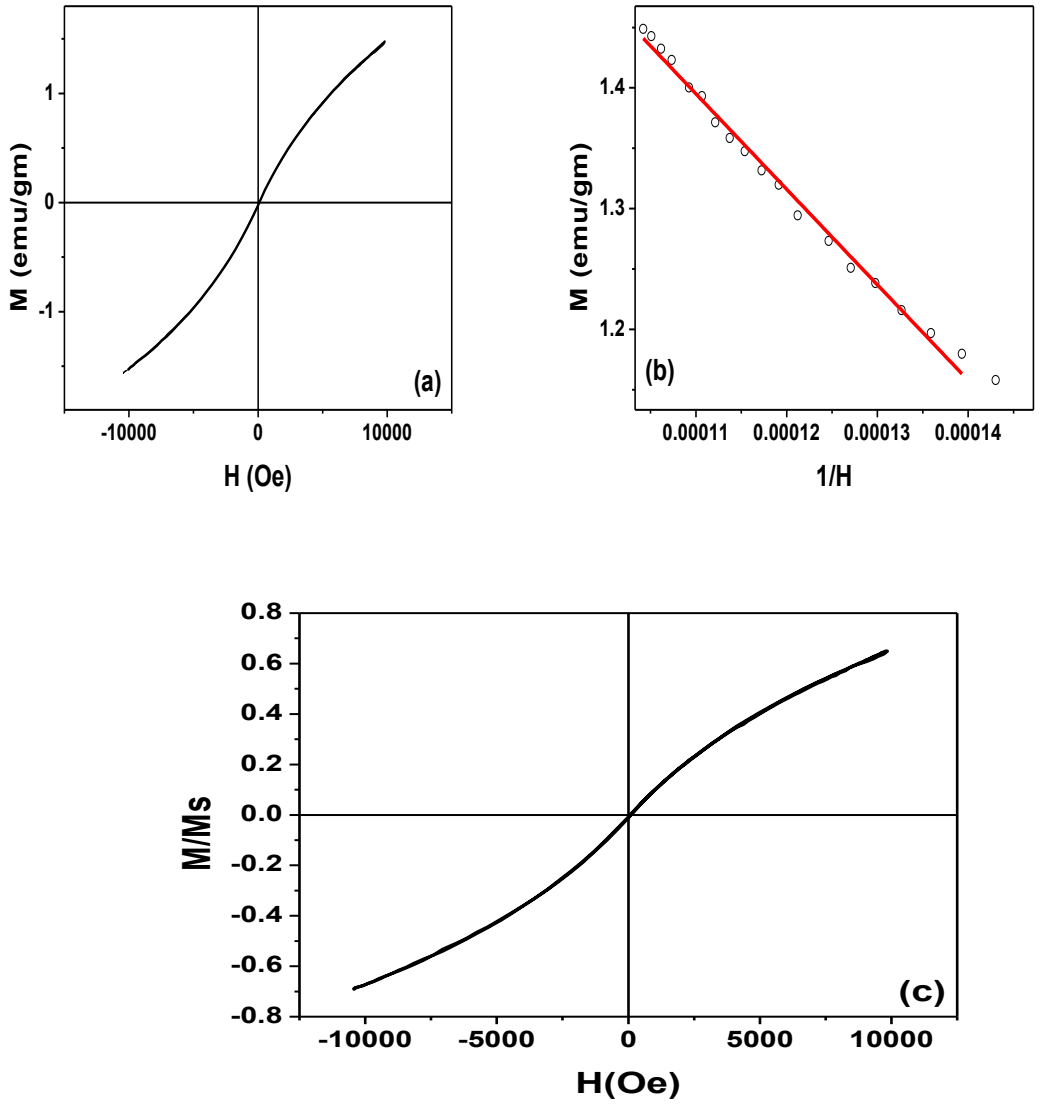

Figure 4.5 (a) M–H hysteresis **(b)** M–1/H and **(c)** M/Ms–H curves of $Mn_{0.4}Zn_{0.6}Fe_2O_4$ nanoparticles

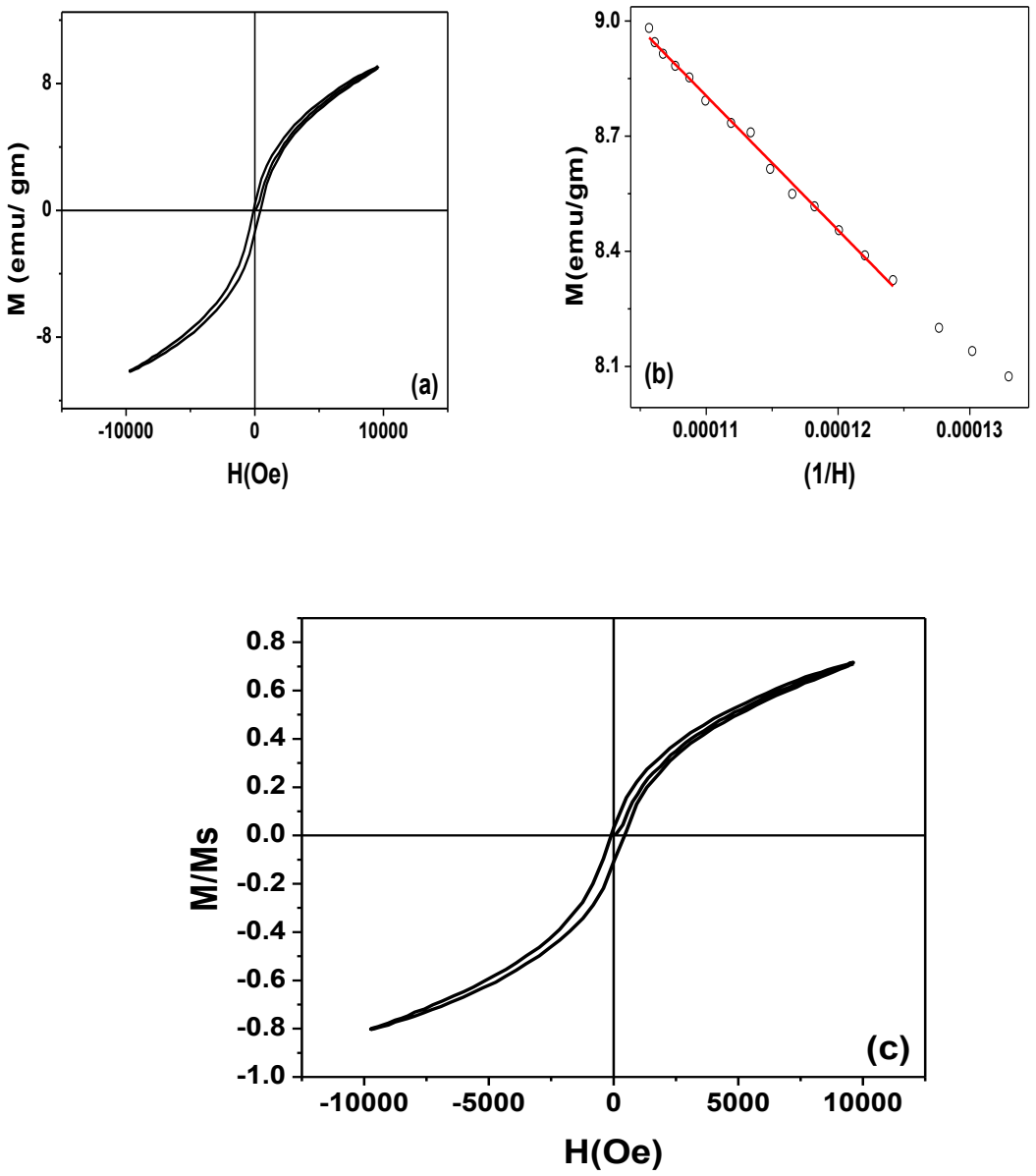

Figure 4.6 (a) M–H hysteresis **(b)** M–1/H and **(c)** M/Ms–H curves of $Mn_{0.2}Zn_{0.8}Fe_2O_4$ nanoparticles

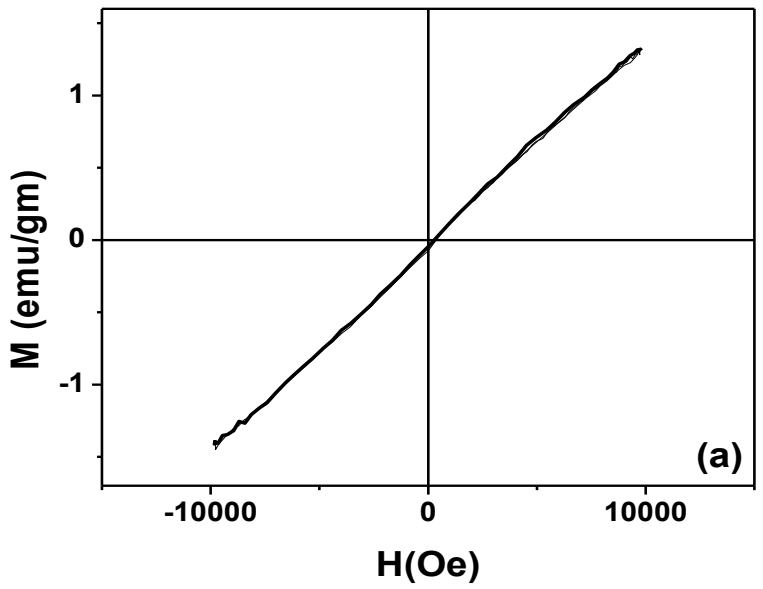

Figure 4.7 M–H hysteresis curve of $ZnFe_2O_4$ nanoparticles

Table 4.2 Saturation magnetization of $Mn_XZn_{(1-x)}Fe_2O_4$ where X (0,0.2, 0.4, 0.6, 0.8, 1) nanoparticles obtained from the VSM measurement.

Sr. No.	Sample Code	Saturation Magnetization(Ms)
1	$MnFe_2O_4$	48.28
2	$Mn_{0.8}Zn_{0.2}Fe_2O_4$	40.91
3	$Mn_{0.6}Zn_{0.4}Fe_2O_4$	29.00
4	$Mn_{0.4}Zn_{0.6}Fe_2O_4$	2.26
5	$Mn_{0.2}Zn_{0.8}Fe_2O_4$	12.65
6	$ZnFe_2O_4$	–

Magnetic properties of bare and functionalized nanoparticles were investigated on PAR VSM. The measurements were carried out at room temperature. For measurement of magnetic properties sample fill in quartz tube and this tube must be fit between the pole pieces of the magnet. Minimum sample required for VSM measurement is 100 mg.

Figure 4.2 (a) shows the M-H curve of $MnFe_2O_4$ nanoparticles recorded at room temperature in the field range of -10 KO_e - +10 KO_e. As observed in the diagram, no

hysteresis is found confirming the superparamagnetic nature of $MnFe_2O_4$ nanoparticles which was predicated from the crystallite size measurement from X- ray diffraction studying. As can be observed from the figure 4.2 (a), the residual magnetization of the sample is zero. Further, no coercive field is required to demagnetize these nanoparticles, which further strengthen our claims that the as-synthesized nanoparticles are superparamagnetic in nature.

In order to determine the saturation magnetization of as-synthesized $MnFe_2O_4$ nanoparticles M- 1/H curve is plotted in the saturation zone. From the linear fit of this data in figure 4.2(b), the saturation magnetization of $MnFe_2O_4$ nanoparticles is determined, which is shown in table 4.2. The observed saturation magnetization of 48.28 emu/g is lower than that reported for bulk $MnFe_2O_4$ (80 emu/g). The reason for decreased in observed saturation magnetization is due to increase in surface to volume ratio with decrease in particle size compared to bulk and also due to the magnetic dead layer present on the surface of magnetic nanoparticles.[32]. The plot of M/Ms is also shown for $MnFe_2O_4$ nanoparticles in figure 4.2(c). The saturation is close to 1.0 which is also an indication of superparamagnetic nature of particles. Figure 4.3 (a) shows the M–H curve for $Mn_{0.8}Zn_{0.2}Fe_2O_4$ nanoparticles along with the corresponding curve of M–1/H and M/Ms-H in figure 4.3(b) and 4.3(c), respectively. Again superparamagnetic nature of nanoparticles is evidenced from the M–H curve. The saturation magnetization of nanoparticles is 40.91 emu/g, which is also reported in table 4.2. The decrease in saturation magnetization is due to their increased non magnetic contribution from Zn. Further, increase in Zn reduces the saturation magnetization of nanoparticles which is evidenced from gradually rising M-H curve in figure 4.4, 4.5, 4.6, and 4.7. The corresponding value of saturation magnetization for each as-synthesized sample is reported in table 4.2. In case of $ZnFe_2O_4$, a linear M-H curve is observed, which is the typical characteristic of a paramagnetic system is. A little hysteresis can also be observed in M-H curve, where the Zn content is increased above 0.4 indicating the formation of ferrimagnetic phase. [33].

4.3 TEM ANALYSIS

TEM analysis of as-synthesized nanoparticles has been done on JEOL model GEM 200 high resolution electron microscope. For this purpose, a fine drop of magnetic nanoparticles dispersed in ethanol was placed on a carbon-coated copper grid and ethanol was allowed to evaporate slowly at room temperature. A representative TEM image of $Mn_{0.2}Zn_{0.8}Fe_2O_4$ and $Mn_{0.8}Zn_{0.2}Fe_2O_4$ nanoparticles along with their electron diffraction images are presented in figure 4.8 and 4.9 respectively. Spherical nature of particle can be observed. Agglomeration

of nanoparticles is also evidenced due to the magnetic nature of the nanoparticles. It is very hard to analysis the micrograph and determines physical size of nanoparticles because of the agglomeration. [32]

Table 4.3 Comparison of crystallite size and physical size of nanoparticles measurement obtained from XRD and TEM

Sr. No.	Samples	Crystallite size (nm)	Physical Size (nm)
1	$Mn_{0.2}Zn_{0.8}Fe_2O_4$	10.4	11.8
2	$Mn_{0.8}Zn_{0.2}Fe_2O_4$	13	9.8

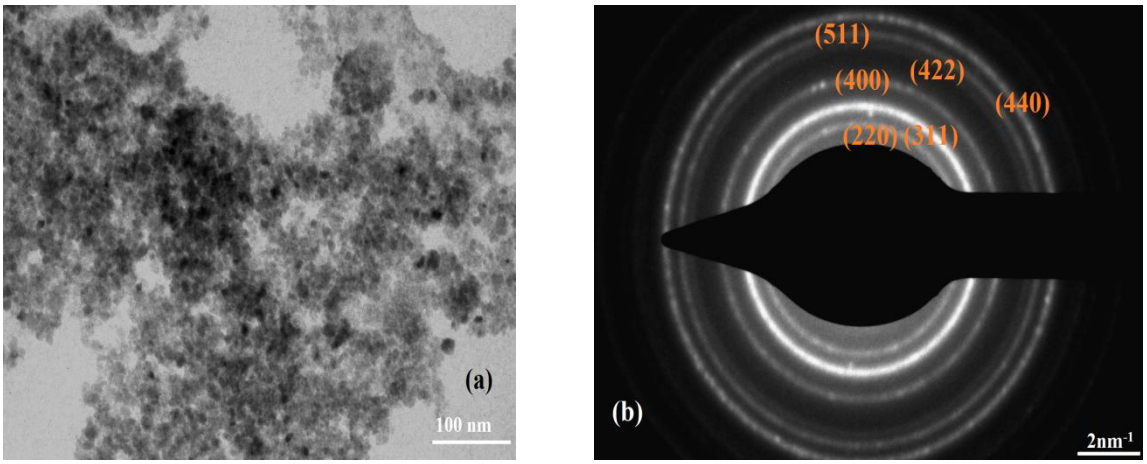

Figure 4.8 (a) TEM image and **(b)** electron diffraction image of $Mn_{0.2}Zn_{0.8}Fe_2O_4$ nanoparticles

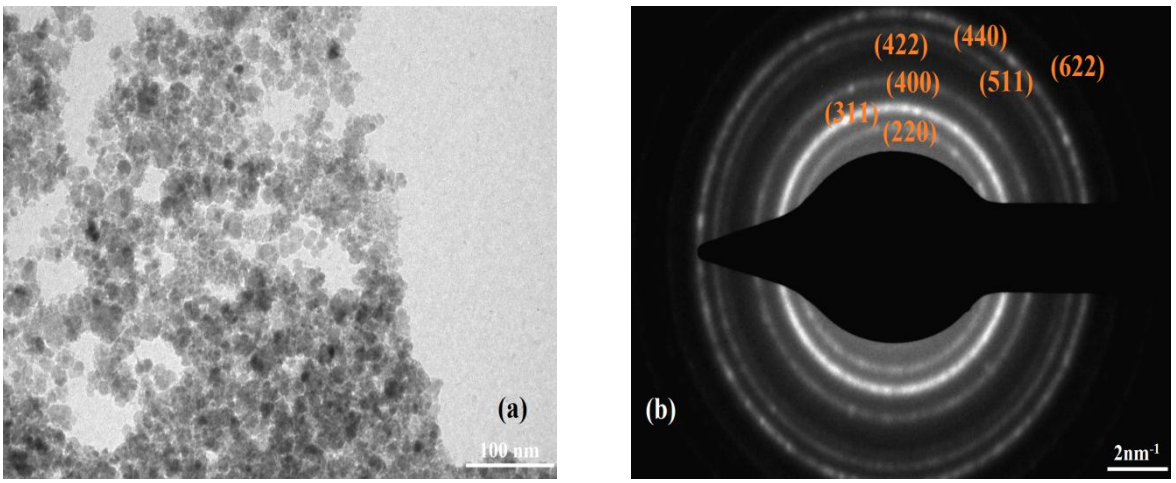

Figure 4.9 (a) TEM image and **(b)** electron diffraction image of $Mn_{0.8}Zn_{0.2}Fe_2O_4$ nanoparticles

The electron diffraction images are analyzed and indexing in figure 4.8 and 4.9. The indexing is in well agreement with the X-ray diffraction analysis. Further, formation of diffraction rings, indicating the poly crystalline nature of magnetic nanoparticles. A comparison chart of crystallite and physical particle size is also presented in table 4.3. Both sizes are in the range of 5-15 nm.

4.4 TGA ANALYSIS

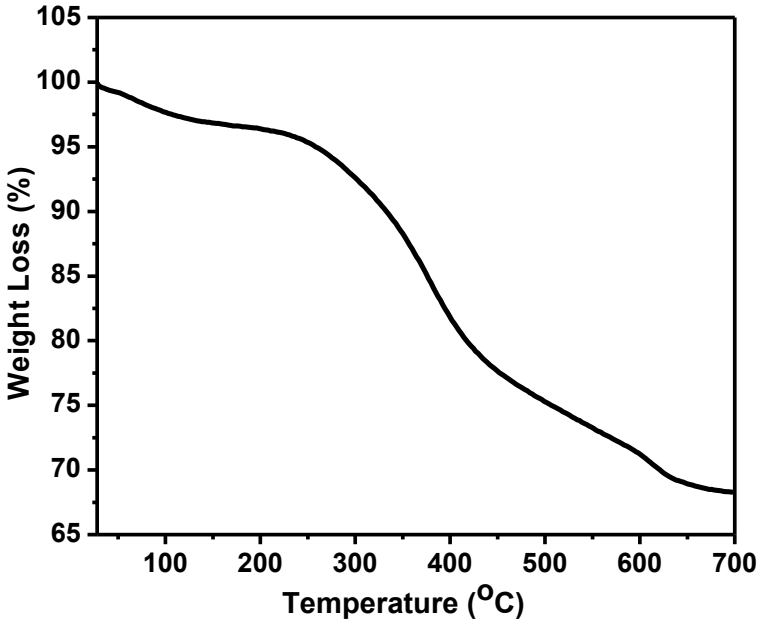

Figure 4.10 TGA curve of oleic acid coated $MnFe_2O_4$ nanoparticles

Figure 4.10 shows the TGA curve of $MnFe_2O_4$ nanoparticles coated with oleic acid. For TGA measurement, nanoparticles of oleic acid coated $MnFe_2O_4$ are dried from the kerosene based magnetic fluid. The TGA curve shows a continues weight loss of 32 % in the temperature range of 30-700°C. This corresponds to their decomposition of oleic acid from the surface of nanoparticles. The observed weight loss is in well agreement with reported by other groups. 32% weight loss is also in good agreement for a monolayer coating of oleic acid on the surface of nanoparticles, which is crucial for the stability of nanoparticles in magnetic fluid [34].

CONCLUSIONS

- $Mn_XZn_{(1-X)}Fe_2O_4$ (x = 0, 0.2, 0.4, 0.6, 0.8, 1.0) nanoparticles are prepared by chemical coprecepitation method. Experimental conditions like reaction temperature, reaction time, reactant concentration, pH, etc have been optimized to produce magnetic nanoparticles with desired properties.
- X-ray analysis confirms that each composition of $Mn_XZn_{(1-X)}Fe_2O_4$ (x =0, 0.2, 0.4, 0.6, 0.8, 1.0) nanoparticles crystallizes into single inverse spinel phase. No impurity or secondary phase is evidenced in the x-ray study.
- To study the particle size of nanoparticles transmission electron microscopy was employed. Highly agglomerated nanoparticles are observed in the TEM images with spherical or near spherical morphologies with average particle size in the range of 7-15 nm. This size is in well agreement with the crystallite size obtained from the x-ray analysis, indicating the formation of single domain magnetic nanoparticles.
- Magnetic nature of nanoparticles was confirmed via VSM study. The magnetic measurement confirms the formation of superparamagnetic nanoparticles of $M_nXZn_{(1-X)}Fe_2O_4$ when $x < 0.4$. For $x > 0.4$, ferrimagnetic nature of nanoparticles is evidenced from the non zero coercieve field and remanant magnetization. The saturation magnetization of nanoparticles decreases with increasing Zn content and it is also lower than the corresponding value in its bulk phase: this decrease in M_s value is attributed to the presence of magnetic dead layer, enhanced surface to volume ratio and increased paramagnetic contribution from Zn.
- TGA study confirms the formation of a monolayer of oleic acid on the surface of Mn-Zn ferrite nanoparticles. This monolayer of oleic acid suppresses the magnetic interaction between the nanoparticles and enhanced fluid stability.
- The knowledge generated here might be useful in producing magnetic nanoparticles for temperature sensitive magnetic fluids used in heat transfer devices.

SCOPE FOR FUTURE WORK

- Magnetic properties of Mn-Zn ferrite nanoparticles were studied only at room temperature in the present study. However, the study of temperature dependent magnetic properties of these nanoparticles is very crucial these nanoparticles are found application of divated temperature.
- Determination of Curie and Neel temperature of as-synthesized magnetic nanoparticles is critical for their application in heat transfer devices.
- Synthesis condition and appropriate surfactant needs to be established for dispersing these nanoparticles in transformer oil.
- Evaluation of thermal and dielectric properties of transformer oil based magnetic fluid is essential before its application in high power transformers.

REFERENCES

[1] Feymann, R.; Annual meeting of American physics society, Journal of Caltech engineering and science, Vol. 23, Issue 5, (1960), pp. 22-36.

[2] Drexler, K.E.; A handbook on engine of creation, The coming era of nanotechnology, doubleday publication, ISBN 0-385-199973-2, (1986), pp. 37-42.

[3] A roundtable conference on apply nanotechnology industry, agri output, The Daily star (Bangladesh), (2012).

[4] Keffer, F; A handbook on the properties of magnetic material, Scientific American, Vol.217, Issue 3, (1967), pp. 222-234.

[5] Gittleman, J. I; Abeles, B., Superparamagnetism and relaxation effects in granular Ni-Sio_2 films, Journal of American physical society, Vol. 9, Issue 9, (1974), pp. 3891-3897.

[6] Albrecht. T; Buchrer, C., First observation of ferromagnetic and ferrimagnetic domain in liquid metal, Journal of applied physics a material science and processing, Vol. 65, Issue 2, (1997), pp. 215-220.

[7] Carter, C; Norton, M., A book on Ceramic material science and engineering, Springer publisher, ISBN 978-0-387-46271-4, vol. 22, (2007), pp. 601-612.

[8] Arulmurugna, R; Vaidnathan, G; Sandilnathan, S,; Jeyadevan,B., Mn-Zn nanoparticle for ferrofluid preparation, Journal of magnetism and magnetic material, Vol. 298, Issue 2, (2006), pp. 83-94

[9] Roberta, L.M; Ronald, C.P; Brian, K.H; Temperature distribution of cation disorder in MgAl2O4 spinal using Al and O magic angle spinning NMR, Journal of American mineralogist, Vol. 77, (1992), pp.44-52.

[10] Chinnsamy, C. N; Naryanasamy, N; Ponpandian, N., Mixed spinal structure in NiFe2O4, Physical review B, Vol. 63, Issue 18, (2001), pp. 1-6

[11] Berkovski, B.; Bashotovoy, V., Magnetic fluid and application handbook, Begal house publisher, Vol. 3, Newyork (1996), pp. 15-24.

[12] Auzans, E.; Zins, D.; Blums, E.; Massart, R., Synthesis and properties of Mn-Zn ferrite ferrofluid, Journal of material science, Vol. 34, Issue 5, (1999), pp. 1253-1260.

[13] Raj, K.; Merimac; Ronald, M., Ferrofluid cooled electromagnetic device and improved cooling method, United States patient no. 5462685, (1995).

[14] Pileni, M.P., Magnetic fluid: fabrication, magnetic properties, and organization of nanocrystals, Journal of advance function and material, Vol. 11, Issue 5, (2001), pp. 323-336.

[15] Voit, W; Kim, D.K.; Zabka, W.; Muhammed, M. and Rao, K.V., Magnetic behavior of coated superparamagnetic iron oxide nanoparticles in ferrofluids, Y7.8.1-Y7.8.7, (2001), pp. 676-683

[16] Grob, C.; Buscher, K.; Romanus, E.; Helm, C.A.; Weitschies, W., Characterization of ferrofluid by atomic force microscopy and photon correlation microscopy after magnetic fractation, Journal of European cells and materials, Vol. 3, Issue 2, (2002), pp.163-166.

[17] Patel, R.; Upadhyay, R.V.; Mehta, R.V., Rheology of transformer based oil ferrofluid, Indian journal of engineering material and sciences, Vol. 11, (2004), pp. 301-304.

[18] Kim, K.D.; Kim, S.S.; Choa, Y.H.; Kim, H.T., Formation and surface modification of Fe_3O_4 nanoparticles by co-precipitation and sol-gel method, Journal of industrial engineering and chemistry, Vol.13, Issue 7, (2007), pp. 1137-1141.

[19] Maity, D.; Aggrawal, D.C., Synthesis of iron oxide nanoparticles under oxidizing environment and their stabilization in aqueous and non-aqueous media, Journal of magnetism and magnetic material, Vol. 308, Issue 1, (2007), pp. 46-55.

[20] Zhan, M.; Magnetic fluid and nanoparticle application to nanotechnology, Journal of nanoparticle research, Vol. 3, (2001), pp. 73-78.

[21] Desai, R.; davariya, V.; Parrekh, K.; Upahdyay, R.V., Structural and magnetic properties of size controlled Mn0.5Zn0.5Fe2O4 nanoparticles and magnetic fluid, Journal of physics, Vol. 73, Issue 4, (2009), pp. 765-780.

[22] Li, Z.; Kawashita, M.; Matusi, N.; Araki, N.; Mitsumori, M.; Hiraoka, M,; Doi, M.; Prepration of magnetic iron oxide nanoparticles for hyperthermia of cancer in Fecl2-$NaNO_3$-NaOH aqueos system, Journal of biometer application, Vol.25, Issue 7, (2011), pp. 643-661.

[23] Ilahi, E.; Zahira, R.; Mehmood, K.; Jamil, A.; Amin, N., Coprecepitation synthesis physical and magnetic properties of Mn ferrite powder, African journal of pure and applied chemistry, Vol. 6, Issue 1, (2012), pp. 1-5.

[24] Kopcansky, P.; Tomaovicso, N.; Koneracka, M; Timco, M.; Zavisova, V.; Toamco, L., Magnetic nanoparticles in magnetic fluid, Journal of acta electrotechnica et informatica, Vol.10, Issue 3, (2010), pp. 10-13.

[25] Mackkenzie, J.D., Application of Sol-Gel process, Journal of non crystalline solid, Vol. 100, Issue 3, (1998), pp. 162-168.

[26] Jonge, H.P.; Sudrashan, T.S., Introduction to chemical vapour deposition, empetak inc., ISBN 0-87170-734-4, Vol. 2, (1955).

[27] Charles, S.W., The preparation of magnetic fluid, Springer verleg Berlin Heidelberg, LNP 594, (2002), pp. 3-18.

[28] Klug, H. P.; and Alexander; L.E., X-ray diffraction procedures for polycrystalline and amorphous materials, Wiley, New York, 2nd ed., (1974).

[29] Foner, S., Versatile and sensitive vibrating sample magnetometer, Journal of physics review of scientific instrument, Vol.30, Issue 7, (1959), pp. 548-557.

[30] William, D.B; and Carter, B., Transmission electron microscope: a text book of material science, Springer US, ISBN 978-0-306-45324-3, (1996), pp. 3-17.

[31] Mansfield, E.; Kar, A.; Quinn, T. P.; Hooker, S. A., Quartz Crystal Microbalances for Microscale Thermogravimetric Analysis, Journal of analytical chemistry, Vol. 82, Issue 24, (2010), pp. 9977-82.

[32] Chudasama, B.; Vala, A.K.; Andhariya, N.; Upadhay, R.V.; Mehta, R.V, Antifungal activity of multifunctional Fe3O4-Ag nanoparticles, Journal of magnetism and material, Vol. 323, (2011), pp. 1233-1237.

[33] Verma, K.C.; Singh, V.P.; Ram, M.; Shah, J; Kotnala, R.K., Structure, microstructural, and magnetic properties of NiFe2O4, CoFe2O4 and MnFe2O4 nanoferrite thin films, Journal of magnetism and magnetic material, Vol. 323, (2011), pp. 3271-3275.

[34] Andhariya, N.; Chudasama, B.; Mehta, R.V.; Upadhyay, R.V., Biodegradable thermoresponsive polymeric magnetic nanoparticles: a new drug delivery plateform for doxorubicin, Journal of nanoparticle research, Vol.13, (2011), pp. 1677-1688.